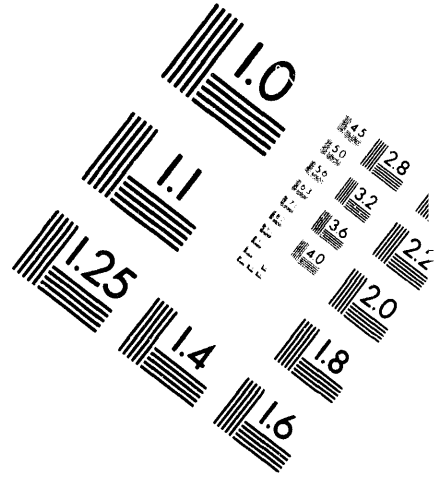
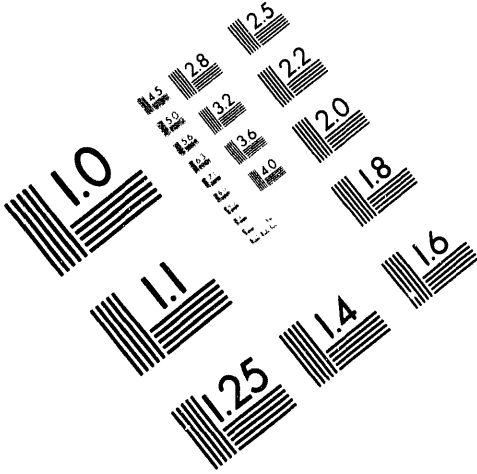




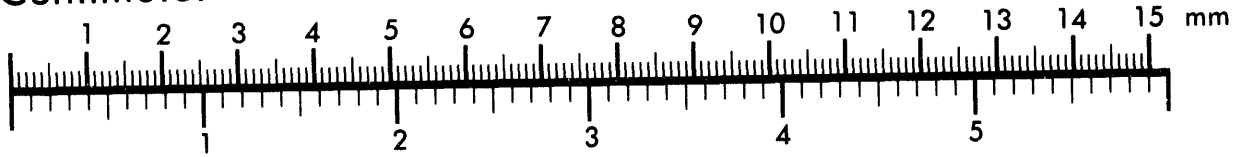
AIM

Association for Information and Image Management

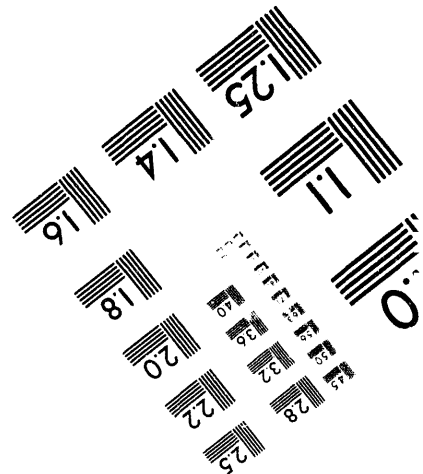
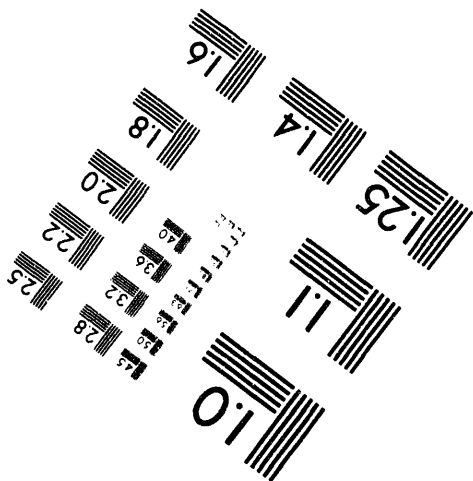
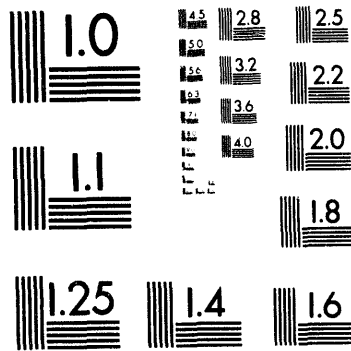
1100 Wayne Avenue, Suite 1100
Silver Spring, Maryland 20910
301/587-8202



Centimeter



Inches



MANUFACTURED TO AIM STANDARDS
BY APPLIED IMAGE, INC.

1 of 1

Conf - 930902 - 1

[Note: This is a preprint of a document submitted for publication. Contents of this document should not be quoted or referred to without permission of the author(s).]

To be presented at the 9th International Conference on Solid State Ionics,
The Hague, the Netherlands, September 12-17, 1993 and published in
Solid State Ionics

RECHARGEABLE THIN-FILM LITHIUM BATTERIES

J. B. Bates, G. R. Gruzalski, N. J. Dudney, C. F. Luck, Xiaohua Yu
Oak Ridge National Laboratory
Oak Ridge, Tennessee 37831-6030

"The submitted manuscript has been authored by a contractor of the U.S. Government under contract No. DE-AC05-84OR21400. Accordingly, the U.S. Government retains a nonexclusive, royalty-free license to publish or reproduce the published form of this contribution, or allow others to do so, for U.S. Government purposes."

DISCLAIMER

This report was prepared as an account of work sponsored by an agency of the United States Government. Neither the United States Government nor any agency thereof, nor any of their employees, makes any warranty, express or implied, or assumes any legal liability or responsibility for the accuracy, completeness, or usefulness of any information, apparatus, product, or process disclosed, or represents that its use would not infringe privately owned rights. Reference herein to any specific commercial product, process, or service by trade name, trademark, manufacturer, or otherwise does not necessarily constitute or imply its endorsement, recommendation, or favoring by the United States Government or any agency thereof. The views and opinions of authors expressed herein do not necessarily state or reflect those of the United States Government or any agency thereof.

SOLID STATE DIVISION
OAK RIDGE NATIONAL LABORATORY
Managed by
MARTIN MARIETTA ENERGY SYSTEMS, INC.
under
Contract No. DE-AC05-84OR21400
with the
U.S. DEPARTMENT OF ENERGY
Oak Ridge, Tennessee 37831-6030

September 1993

MASTER

EP

CONFIDENTIAL - NOT FOR DISTRIBUTION

RECHARGEABLE THIN-FILM LITHIUM BATTERIES

J. B. Bates, G. R. Gruzalski, N. J. Dudney, C. F. Luck, Xiaohua Yu
Oak Ridge National Laboratory
Oak Ridge, Tennessee 37831-6030

Abstract

Rechargeable thin-film batteries consisting of lithium metal anodes, an amorphous inorganic electrolyte, and cathodes of lithium intercalation compounds have been fabricated and characterized. These include Li-TiS₂, Li-V₂O₅, and Li-Li_xMn₂O₄ cells with open circuit voltages at full charge of about 2.5 V, 3.7 V, and 4.2 V, respectively. The realization of these robust cells, which can be cycled thousands of times, was possible because of the stability of the amorphous lithium electrolyte, lithium phosphorus oxynitride. This material has a typical composition of Li_{2.9}PO_{3.3}N_{0.46} and a conductivity at 25°C of 2 μS/cm. The thin-film cells have been cycled at 100% depth of discharge using current densities of 5 to 100 μA/cm². Over most of the charge-discharge range, the internal resistance appears to be dominated by the cathode, and the major source of the resistance is the diffusion of Li⁺ ions from the electrolyte into the cathode. Chemical diffusion coefficients were determined from ac impedance measurements.

Introduction

The idea of a rechargeable thin-film battery based on a lithium anode and an intercalation cathode is an old one. At the 1983 SSI conference in Grenoble, Kanehori and co-workers [1] reported the fabrication of such a battery having an amorphous lithium phosphosilicate electrolyte, with a reported composition of Li_{3.6}Si_{0.6}P_{0.4}O₄, and a TiS₂ cathode. The battery had an open circuit voltage of about 2.5 V at full charge, and one of the cells was cycled 2000 times at current densities of up to 16 μA/cm². At the same conference, Levasseur and colleagues [2] reported on a solid state battery they fabricated by depositing 1-μm-thick lithium borosilicate electrolyte film onto a TiS₂ pellet followed by evaporation of a lithium anode film. Later, this group described the fabrication of rechargeable thin-film lithium cells

using a titanium oxysulfide cathode, a $\text{Li}_2\text{O-B}_2\text{O}_3\text{-Li}_2\text{SO}_4$ electrolyte, and a lithium anode [3]. Up to 50 cycles were obtained at current densities as high as $62 \mu\text{A}/\text{cm}^2$. In the same year, Creus et al. reported [4] on their thin-film lithium batteries with open circuit voltages of up to 3.1 V. These cells consisted of amorphous $\text{V}_2\text{O}_5\text{-TeO}_2$ cathodes, amorphous $\text{Li}_2\text{S-SiS}_2\text{-P}_2\text{S}_5$ electrolytes, and lithium anodes. These researchers noted that the poor performance of their cells was evidently due to the reaction between lithium and the electrolyte. This problem was alleviated to some extent by depositing a layer of LiI on the electrolyte to serve as a buffer between the electrolyte and the lithium anode. This technique of protecting the electrolyte with a layer of LiI deposited between the electrolyte film and the anode film was successfully used by Jones and colleagues at Eveready Battery Co. [5,6] to develop thin-film Li-TiS_2 batteries with excellent performance over thousands of charge-discharge cycles. Several of the Eveready cells have undergone more than 10,000 cycles at current densities of up to $100 \mu\text{A}/\text{cm}^2$ with little change in performance, while others stored at room temperature for nearly two years have retained 98% of their initial voltage. However, the LiI layer further complicates cell fabrication, and it also limits the cathodes which can be used due its restricted stability window of about 2.8 V [7].

Recently, we reported the discovery [8,9] of a new amorphous lithium electrolyte, lithium phosphorus oxynitride, that is stable at high cell potentials. Using this electrolyte, thin-film rechargeable lithium batteries with $\text{Li}_x\text{Mn}_2\text{O}_4$, TiS_2 , and V_2O_5 cathodes have been fabricated [10]. In addition, some success has been achieved in protecting the lithium anode with a thin-film coating so that cells have been able to survive for several months in air. In this paper, we discuss the fabrication and characterization of these thin-film batteries, emphasizing the $\text{Li-V}_2\text{O}_5$ system.

Cell Fabrication and Characterization

A cross-sectional drawing of a typical thin-film battery is shown in Fig. 1. The cathode illustrated is amorphous vanadium pentoxide (V_2O_5), but it could be any one of several lithium intercalation compounds that can be deposited in thin-film form. The steps for the fabrication of a Li- V_2O_5 cell illustrated in Fig. 2 include:

1. V current collectors—dc magnetron sputtering of V in Ar
2. V_2O_5 cathode—dc magnetron sputtering of V in Ar + 14% O_2
3. Li electrolyte—rf magnetron sputtering of Li_3PO_4 in N_2
4. Li anode—evaporation of Li (10^{-6} Torr)
5. Protective coating

Cells based on TiS_2 and $LiMn_2O_4$ were fabricated in a similar manner using cathodes prepared elsewhere by methods described in the literature [5,6,11].

For the sputter depositions, two-inch magnetrons (Torus) were used. The commercial V target had a specified purity of 99.97%; the Li_3PO_4 target was prepared by pressing Li_3PO_4 powder (Johnson Mathey, 99.9%) into a 2"-diameter \times 1/8"-thick disk and then sintering the disk in air at 900°C for 4 hrs. The substrate was located 5 cm above the targets, and the total pressure during sputtering was 20 mTorr. The cathode and electrolyte depositions were the slowest steps in the fabrication process. Both were deposited at rates of about 0.1 $\mu\text{m/hr}$ using powers of about 30 W (dc) and about 35 W (rf) applied to the V and Li_3PO_4 targets, respectively. Typically the cathode and electrolyte films were each about 1- μm thick. A variety of techniques have been used to characterize the physical and chemical properties of individual cathode and electrolyte films [12,13]. These include Rutherford backscattering spectrometry (RBS), proton induced gamma ray emission spectrometry (PIGE), x-ray

diffraction, scanning electron microscopy (SEM), x-ray microanalysis, x-ray photoelectron and Auger electron spectroscopies, and ac impedance.

The lithium films were deposited at a rate of about 10 $\mu\text{m/hr}$ by evaporation of lithium metal contained in a Ti crucible. The substrate was located a few millimeters above a chimney placed on top of the crucible to minimize Li deposition on the chamber walls and fixtures. The Li films were typically 3- to 5- μm thick corresponding to about five to ten times more lithium required for full discharge of 1- μm -thick V_2O_5 cathode films. All of the operations with lithium were carried out in a recirculating glove box filled with Ar (99.999%), with the O_2 and H_2O content maintained at a few ppm. Prior to starting a series of lithium depositions, the box was purged with Ar to remove any residual N_2 . After deposition of the lithium film, the cells were transferred in Ar to another deposition system where the protective coating was applied.

Laboratory cells typically have an area of about 1 cm^2 and are about 6- μm thick, and they are usually deposited on 1" square glass microscope slides. For cells based on V_2O_5 or TiS_2 cathodes, all depositions are carried out at ambient temperature, so these batteries could be fabricated on virtually any substrate capable of supporting a thin film. For example, Li- V_2O_5 cells have been fabricated on alumina, glass, and 0.1-mm-thick polyester. The LiMn_2O_4 cathode, however, requires [11] a post deposition anneal at 400°C in order to obtain the crystalline spinel phase. Consequently, until a lower temperature deposition process can be found, the selection of substrates onto which Li- LiMn_2O_4 batteries can be fabricated is limited.

Cycling of the thin-film cells was carried out at constant current between specified voltage limits using two Keithley 617 electrometers operated under computer control. At the end of each half-cycle, the voltage was held constant until the current decreased to a specified fraction of the charge or discharge current, usually 10%. The impedance of the cells was measured at 25°C at frequencies from 0.01 Hz

to 10 MHz using methods described elsewhere [13]. These measurements were made at different cell potentials on both charge and discharge cycles. A dc bias equal to the OCV was applied to the cells during the impedance measurements, and the ac voltage was 50 mV or less. The OCV measured before and after the impedance measurements agreed within a few mV.

Results and Discussion

The good performance of the thin-film rechargeable lithium batteries discussed below is due primarily to the electrolyte, an amorphous lithium phosphorus oxynitride, denoted by Lipon. This is a recently synthesized material [8,9] that has a lithium ion conductivity of about 2×10^{-6} S/cm at 25°C, a Li⁺ transport number of unity, and, most importantly, is stable in contact with metallic Li at high-cell voltages. Recent I-V measurements on V/Lipon/V thin-film structures indicate that the decomposition voltage of Lipon is higher than 5 volts. The composition of Lipon, as determined from RBS and PIGE measurements [9], is typically Li_{3.3}PO_{3.8}N_{0.22}, but the N content has been observed to vary from 2 to 6 at.%.

The vanadium oxide films were x-ray amorphous. Their O/V ratios determined from RBS and Auger measurements agreed well: O/V = 2.5 ± 0.1 . The density of the V₂O₅ films has not been accurately determined, but from measurements of film thickness (using a profilometer) and mass (obtained from deposition rates determined with a quartz crystal oscillator), an average density of 3 g/cm³ was obtained from six separate depositions. Kennedy et al. [14] reported that the density of V₂O₅ films grown by evaporation ranged from 2.42 g/cm³ to 2.69 g/cm³. We measured the electronic conductivity of a V₂O₅ film sandwiched between V contacts to be 1.5×10^{-7} S/cm at 25°C. A value of 10^{-6} S/cm was reported for the evaporated thin films [14], and Koffyberg and Benko [15] reported conductivities as high as $4 \times$

10^{-5} S/cm for amorphous V_2O_5 films deposited by sputtering vanadium oxide targets. This latter value is even higher than the conductivity reported [16] for bulk amorphous V_2O_5 , 6.5×10^{-6} S/cm

The TiS_2 cathodes [5] were x-ray amorphous, presumably due to a small crystallite size, and the S/Ti ratio was 2.09. The composition and phase of the crystalline $LiMn_2O_4$ cathode was confirmed by x-ray diffraction [11].

Examples of discharge curves for Li- TiS_2 , Li- V_2O_5 , and Li- $LiMn_2O_4$ cells are shown in Fig. 3. The data are plotted as cell voltage vs. the quantity of charge passed per volume of cathode. The Li- V_2O_5 and Li- TiS_2 cells are deposited in the fully charged state. The first deep discharge of these cells to 1.5 V and 1.8 V, respectively, is represented by



and



On the subsequent charge cycle, about 2.8 Li per V_2O_5 is extracted from the cathode. A comparable capacity loss on the first discharge is also observed when the lower cutoff voltage is 2.7 V. This is illustrated in charge-discharge curves for a Li- V_2O_5 cell in Fig. 4(a), where it can be seen that the quantity of charge passed through the cell on the first discharge is larger than that of the following cycles. A similar effect is found for the Li- TiS_2 cells [6]. This initial large loss in capacity is not well understood, but it has been suggested [17,18] that a discharge below about 2 Li per V_2O_5 in crystalline vanadium oxide induces an irreversible structural change in the cathode forming domains with deep potential wells that trap lithium ions. These ions then are not extracted on subsequent charge cycles. As illustrated in Fig. 5, after the first discharge, there is a slow but continuous decrease in the amount of lithium inserted into and extracted from the cathode, possibly due to further irreversible structural

changes. For cycling to 1.5 V, this capacity loss reaches a level rate of about 0.6% per cycle. If the lower cutoff voltage is increased to 1.8 V, this loss reduces to about 0.1%.

Examples of the charge-discharge curves for a Li-LiMn₂O₄ cell are shown in Fig. 6. The as-deposited cathode has a composition near LiMn₂O₄ [11], and the open circuit voltage of a cell can vary between 3 and 3.9 V depending on the exact lithium content. The battery is first charged to 4.5 V. Assuming that one Li per Mn₂O₄ is extracted from the cathode during this initial charge [11], the subsequent discharge-charge cycles, restricted to the voltage range shown in Fig. 6, should be represented by



However, compared to the amount of cathode deposited, about 0.6 Li per Mn₂O₄ is cycled through the cell after the initial charge. Possibly the assumed quantity of lithium initially extracted from the cathode was too large, but in any case it appears that a significant fraction of the as-deposited cathode becomes "electrochemically inactive" after the initial charge. This suggests an irreversible structural change occurs in the cathode on the initial charge.

The charge-discharge curves are well-behaved provided the lower voltage cutoff does not fall below about 3.6 V. After the first charge, the amount of lithium that can be inserted into the cathode continues to decrease by about 0.1% on each successive cycle. This is shown by the data in Fig. 7 for cycles 30–70, and it indicates that a continuous subtle change in the structure of the cathode occurs with each cycle. If the discharge is extended beyond the cathode composition of LiMn₂O₄ (i.e., Li_{1+x}Mn₂O₄), the cell potential drops abruptly to 3 V indicating the appearance of a second phase. When the discharge voltage was reduced to 3 V after completing 150 cycles of the Li-Li_xMn₂O₄ cell, the films detached from the substrate, possibly due

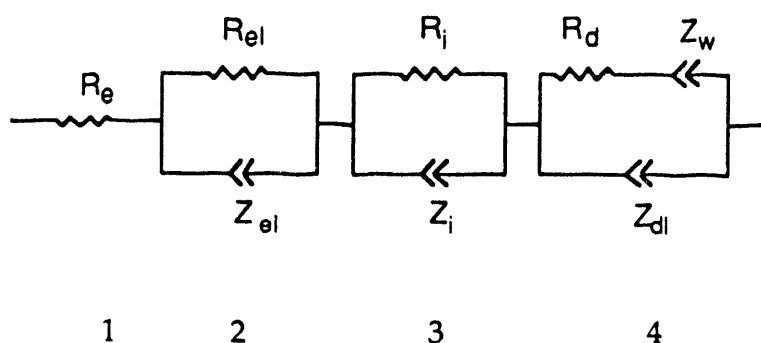
to the nearly 6% increase in unit cell volume that occurs during the phase change [19].

Except for the small loss in cell capacity, all three of the thin-film lithium batteries show no degradation in performance after many charge-discharge cycles. Jones and colleagues [6] have achieved more than 10,000 cycles with some of their Li-TiS₂ cells with little change in cell performance between the first and last cycle. We believe that this unique property of thin-film solid state cells is due to the rigid interfaces between the lithium anode and the electrolyte and between the electrolyte and the cathode. A Li-TiS₂ cell with a Lipon electrolyte was cycled over 4000 times before failing due to a short circuit. The cell was fractured in a glove box and transferred to an SEM under high purity Ar. The micrograph of one of the fracture cross sections displayed in Fig. 8 shows that the interface between the lithium anode and the electrolyte remained smooth. There is no evidence for the formation of lithium dendrites that occurs on cycling of lithium cells having organic liquid or polymer electrolytes. The shelf life of thin-film lithium batteries is also good. We observed no significant change in the open circuit voltage of a Li-V₂O₅ cell stored for more than 12 months.

The energy densities, specific energies, and capacities for the Li-TiS₂, Li-V₂O₅, and Li-Li_xMn₂O₄ thin-film batteries are listed in Table 1. The energy of the cells was determined from the integrals $\int V(q)dq$ over the respective discharge curves (Fig. 3) calculated between the voltages specified in the second column in the table. The mass and volume of the cells were based on 1- μ m-thick cathode and electrolyte films plus an anode film thick enough to provide three times the maximum amount of Li required by the respective cathodes as specified in equations 1-3 above. For the cathodes, the crystalline densities were assumed, although the actual densities of the TiS₂ and V₂O₅ films are lower. This procedure was followed because the density of the LiMn₂O₄ film has not been determined. For the

electrolyte film, the density of 2.4 g/cm^3 reported [20] for a bulk lithium phosphorus oxynitride glass was assumed. If the actual film densities for V_2O_5 and TiS_2 were used, the energy densities would be reduced by about 10%.

Presently, the current density of rechargeable thin-film batteries with $1\text{-}\mu\text{m}$ -thick cathodes is limited to about $100 \mu\text{A/cm}^2$ without an excessive voltage drop due to internal resistance. From impedance data for each of the three types of cells investigated, the diffusion of Li^+ ions from the electrolyte into the cathode is the major source of this resistance over most of the charge-discharge range. Examples of the impedance spectra for two $\text{Li-V}_2\text{O}_5$ cells at two voltages are shown in Fig. 9. The solid curves were obtained by a fit of the equivalent circuit model shown below to the impedance data. The model is constructed from the four components labeled 1-4. The constant phase angle (CPA) elements Z in the circuit



have the form $Z = A(j\omega)^{-n}$ where A and n are constants [21]. Components 1, 2, and 4 represent the electronic resistance of the cathode, the impedance of the electrolyte, and the impedance of the cathode, respectively. The latter was assumed to have the form of Randles' circuit originally proposed to account for the impedance of fast reactions at metal electrodes in electrolyte solutions [22]. In this model, R_d is usually called the charge transfer resistance, Z_w the diffusion impedance, and Z_{dl} the impedance of the double layer at the cathode-electrolyte interface. In Randles

original circuit, a simple capacitor was used to represent the double layer impedance, which is equivalent to setting $n = 1$ in the CPA term, Z_{dl} . As anticipated from prior research [21], a CPA element is required to obtain an acceptable fit to the data. The frequency exponent $n = 1/2$ in the Warburg term, Z_w . The origin of component 3 in the model is not known at this time, but it is associated with the formation of the Lipon- V_2O_5 interface. All four of the equivalent circuit components also appear in the impedance spectra of a V/Lipon/ V_2O_5 /V thin-film structure, so component 3 is not due to the Li-electrolyte interface. Moreover, this component does not appear in the impedance spectra of a Li- $Li_xMn_2O_4$ cell nor that of a Li-TiS₂ cell.

The parameters used to obtain the calculated $Re(Z)$ and $Im(Z)$ shown in Fig. 9(a) are listed in Table 2. Ho et al. [23] extended Randles' model to intercalation cathodes and obtained a relationship between the constant A_w and the chemical diffusion coefficient \tilde{D}_i for the cations in cathode:

$$A_w = \frac{V_m dV/dx}{\sqrt{2} Fa} \cdot \frac{1}{\sqrt{\tilde{D}_i}} \quad (4)$$

where dV/dx is the derivative of the cell potential with the change in the cation stoichiometry parameter, eg. x in $Li_xV_2O_5$, V_m is the molar volume, F is Faraday's constant, and a is the area of the cathode. The diffusion coefficients given in Table 3 were calculated by from Eq. (4) using the fitted values of A_w , $V_m = 54.1 \text{ cm}^3/\text{mol}$ (crystalline value), and $dV/dx = 0.75 \text{ V}$. These are effective diffusion coefficients which include not only the ionic mobility and thermodynamic enhancement factors but also the film microstructure. By comparison, Baudry et al. [24] reported a diffusion coefficient of $2.5 \times 10^{-12} \text{ cm}^2/\text{s}$ for Li^+ ions in V_2O_5 thin films grown by evaporation as determined from impedance measurements on an electrochromic window at 3V/Li.

The term R_d in the Randles circuit is usually referred to as a charge transfer resistance implying both ionic and electronic contributions. In the cells we have investigated, the magnitude of R_d arises solely from the resistance to insertion of Li^+ ions into the cathode with no evident contribution from electron transport. The magnitude of R_d is highest in the fully charged cell and decreases as Li is added to the cathode. Graphs of the cell resistance, denoted by R_{max} , vs. cell voltage for three Li- V_2O_5 cells are shown in Fig. 10. Depending on the particular cell, for example cell 76A, $R_{\text{max}} = R_d$ over most of the discharge range and decreases exponentially with voltage as indicated by the solid line drawn through the data points. For other cells such as 73A and 119A, R_{max} reaches a nearly constant value as R_d becomes comparable to or smaller than R_i , which remains nearly constant over the full discharge range. As the data indicate, R_{max} (R_d) can differ by several orders of magnitude for different cells at high charge states. The decrease in R_{max} (R_d) with decreasing cell voltage shows that the rate limiting step in the transfer of Li^+ from the electrolyte to the cathode is the insertion of Li^+ ions into the V_2O_5 structure: the diffusivity of Li^+ in V_2O_5 increases as the Li^+ content increases (cell voltage decreases). The electronic resistivity is also expected to increase in a similar manner, but we know from the ac and dc measurements on the cathode alone that the electronic conductivity in V_2O_5 is much higher than the ionic conductivity. As indicated in Table 3, the electronic resistivity R_e of the cathode was lower by more than a factor of ten in cell 76A compared to cell 73A.

Conclusions

The rechargeable thin-film lithium batteries described in this paper have high specific energies and energy densities, the ability to undergo thousands of charge-discharge cycles, and they can be fabricated into a variety of sizes and shapes on virtually any type of substrate. The batteries can operate over a wide temperature

range limited at the upper end by the melting point of Li. The useful current density is limited to about $100 \mu\text{A}/\text{cm}^2$ for 1- μm -thick cathodes due to the resistance to insertion of Li^+ ions into cathodes.

Acknowledgments

The authors wish to thank Mr. Steve Jones of Eveready Battery Co. for providing several of the TiS_2 cathodes and for the long cycling of a Li- TiS_2 cell with the Lipon electrolyte. We also thank Dr. F. Shokoohi of Belcore for supplying a thin-film of LiMn_2O_4 that we used in fabricating the Li- $\text{Li}_x\text{Mn}_2\text{O}_4$ battery. Portions of the research were sponsored by the Division of Materials Sciences, U.S. Department of Energy, under contract DE-AC05-84OR21400 with Martin Marietta Energy Systems, Inc.

References

1. K. Kanehori, K. Matsumoto, K. Miyauchi, and T. Kudo, *Solid State Ionics*, 9&10, 1445 (1983).
2. A. Levasseur, M. Kbala, P. Hagenmuller, G. Couturier, and Y. Danto, *Solid State Ionics*, 9&10, 1439 (1983).
3. G. Meunier, R. Dormoy, and A. Levasseur, *Mater. Sci. and Eng.* B3, 19 (1989).
4. R. Creus, J. Sarradin, R. Astier, A. Pradel, and M. Ribes, *ibid.*, B3, 109 (1989).
5. S. D. Jones, J. R. Akridge, S. G. Humphrey, C.-C. Liu, and J. Sarradin, p. 31, *MRS Symposium Proceedings*, Vol. 210, edited by G.-A. Nazri, D. F. Shriver, R. A. Huggins, and M. Bulkanski, Materials Research Society, Pittsburgh, Pennsylvania, 1990.
6. S. D. Jones and J. R. Akridge, *J. Power Sources*, 43-44, 505 (1993).
7. R. A. Huggins in *Proceedings of the Symposium on Lithium Batteries*, ed. by A. N. Dey (The Electrochemical Society, Pennington, NJ, 1987), Vol 87-1, p. 356.
8. J. B. Bates, G. R. Gruzalski, N. J. Dudney, and C. F. Luck, p. 337, *Proc. 35th Power Sources Symposium* (1992).

9. J. B. Bates, N. J. Dudney, G. R. Gruzalski, R. A. Zuhr, A. Choudhury, C. F. Luck, and J. D. Robertson, *J. Power Sources*, 43-44, 103 (1993).
10. J. B. Bates, G. R. Gruzalski, N. J. Dudney, C. F. Luck, X.-H. Yu, and S. D. Jones, *Solid State Technology*, 36, 59 (1993).
11. F. K. Shokoohi, J. M. Tarascon, B. J. Wilkens, D. Guyomard, and C. C. Chang, *J. Electrochem. Soc.*, 139, 1845 (1992).
12. J. B. Bates, N. J. Dudney, C. F. Luck, B. Sales, and R. Zuhr, *J. Am. Ceram. Soc.*, 74, 929 (1993).
13. J. B. Bates, N. J. Dudney, G. R. Gruzalski, R. A. Zuhr, A. Choudhury, C. F. Luck, and J. D. Robertson, *Solid State Ionics*, 53-56, 647 (1992).
14. T. N. Kennedy, R. Hakim and J. D. Mackenzie, *Mat. Res. Bull.*, 2, 193 (1967).
15. F. P. Koffyberg and F. A. Benko, *Phil. Mag.* 38, 357 (1978).
16. C. Sanchez, R. Morineau, and J. Livage, *Phys. Stat. Sol.*, 76, 661 (1983).
17. S. Hub, A. Tranchant, and R. Messina, *Electrochem. Acta*, 33, 997 (1988).
18. C. A. Cartier, A. Tranchant, M. Verdaguer, R. Messina, and H. Dexpert, *Electrochem. Acta*, 35, 889 (1990).
19. T. Ohzuku, M. Kitagawa, and T. Hirai, *J. Electrochem. Soc.*, 137, 769 (1990)
20. L. Boukbir and R. Marchand, *Rev. Chim. Min.*, 23, 343 (1986).
21. J. B. Bates, J.C. Wang, and Y. T. Chu, *J. Non-Cryst. Solids* 131-133, 1046 (1991).
22. J. E. B. Randles, *Disc. Faraday Soc.* 1, 11 (1947).
23. C. Ho, I. D. Raistrick, and R. A. Huggins, *J. Electrochem. Soc.* 127, 343 (1980).
24. P. Baudry, M. A. Aegerter, D. Deroo, and B. Valla, *J. Electrochem. Soc.* 138, 460 (1991).

Table 1. Comparison of three types of rechargeable thin-film lithium batteries.

Cathode	Voltage (V)	Capacity	Energy Density ^a (Wh/l)	Specific Energy (Wh/kg)
		($\mu\text{Ah}/\text{cm}^2\text{-}\mu\text{m}$)		
TiS ₂	2.45–1.8	75	364	225
V ₂ O ₅	3.7–1.5	123	611	444
Li _x Mn ₂ O ₄	4.2–4.0	40	433	211

^aBased on the combined mass of the lithium anode at three times overcapacity, the electrolyte film 1- μm thick, and the cathode. Crystalline densities of the cathodes assumed to calculate the volume of the cells.

Table 2. Parameters of the equivalent circuit for Li-V₂O₅ thin-film cells obtained by a least-squares fit to the measured impedance.

	Cell 76A (3.54 V)	Cell 73A (3.6 V)
A_w	2648	1702
n_w	0.5	0.5
$R_d(\Omega)$	9.6×10^4	4.6×10^3
A_{dl}	5.1×10^4	2.2×10^4
n_{dl}	0.64	0.85
A_{el}	3.1×10^6	6.7×10^6
n_{el}	0.81	0.85
$R_{el}(\Omega)$	50	40
A_i	2.4×10^5	4.6×10^5
n_i	0.85	0.77
$R_i(\Omega)$	1306	3615
$R_e(\Omega)$	10	153

Table 3. Chemical diffusion coefficients \tilde{D}_{Li} for Li^+ ions in V_2O_5 cathodes as a function of Li content: $\text{Li}_x\text{V}_2\text{O}_5$

$\text{Li}_x\text{V}_2\text{O}_5$					
Cell 76A			Cell 199A		
$V_o(\text{V})$	x	$\tilde{D}_{\text{Li}}(\text{cm}^2/\text{s})$	$V_o(\text{V})$	x	$\tilde{D}_{\text{Li}}(\text{cm}^2/\text{s})$
3.4	0.29	4×10^{-15}	3.5	0.14	2.7×10^{-14}
2.6	1.4	2.6×10^{-13}	2.6	1.4	1.3×10^{-12}
1.8	2.6	2.6×10^{-12}	1.6	2.9	1.6×10^{-12}

$V_m = 54.1 \text{ mol/cm}^3, dV/dx = 0.75\text{V}$

Figure Captions

Fig. 1. Schematic cross section of a thin-film lithium battery.

Fig. 2. Deposition sequence and typical geometry of a thin-film lithium battery.

Fig. 3. Discharge curves for three types of thin-film batteries.

Fig. 4. (a) Examples of the first discharge to 2.7 V and first few cycles of a Li-V₂O₅ cell. (b) Example of a deep discharge curve

Fig. 5. The charge inserted into a V₂O₅ cathode as a function of the cycle number for cycling between 3.5 V and 1.5 V.

Fig. 6. Several charge-discharge curves for a Li-Li_xMn₂O₄ cell following the initial charge.

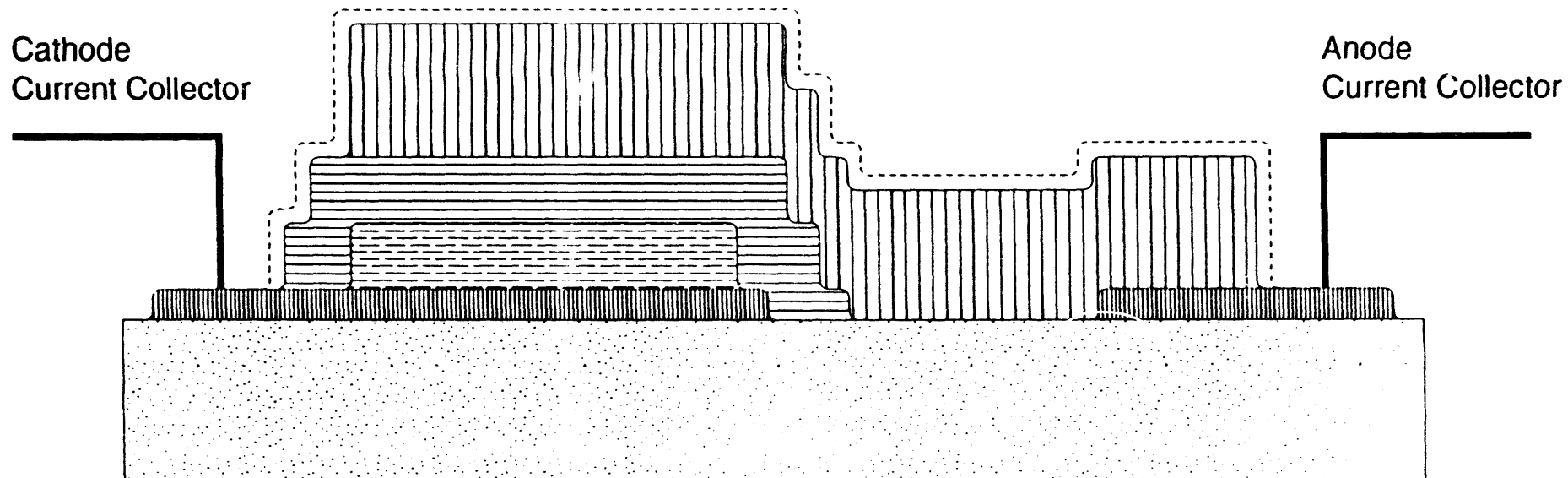
Fig. 7. The charge inserted into a Li_xMn₂O₄ cathode as a function of the cycle number.

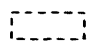

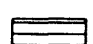
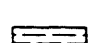

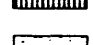
Fig. 8. SEM micrograph of a fracture cross section of a Li-TiS₂ cell after more than 4000 cycles.

Fig. 9. Impedance of two Li-V₂O₅ cells. (a) At nearly full charge. (b) After discharge to a lower voltage. The solid curves were obtained from a fit of the equivalent circuit model (see text) to the measured impedance.

Fig. 10. Cell resistance R_{\max} as a function of cell voltage for three Li-V₂O₅ cells.

Li / V₂O₅ Rechargeable Thin-Film Battery



-  Protective Coating
-  Li
-  Li⁺ electrolyte
-  V₂O₅
-  V
-  Substrate


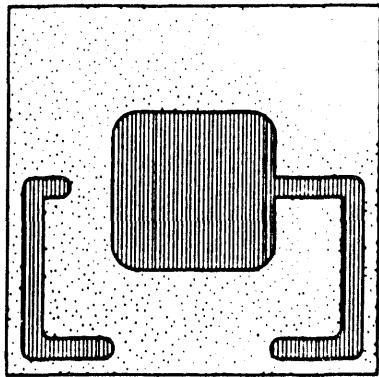
 ~ 2 μm

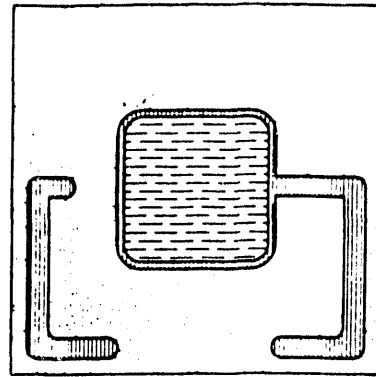
Fig. 1

Li / V₂O₅ Rechargeable Thin-Film Battery



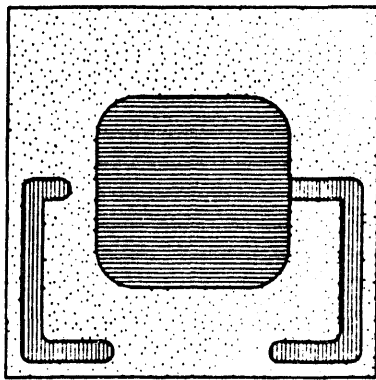
1

Vanadium geometry



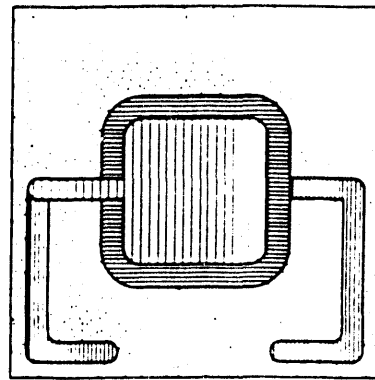
2

V₂O₅ / V



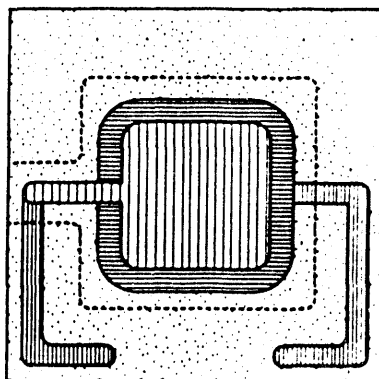
3

Li⁺ electrolyte / V₂O₅ / V



4

Li / Li⁺ electrolyte / V₂O₅ / V



5

Protective Coating

Fig. 2

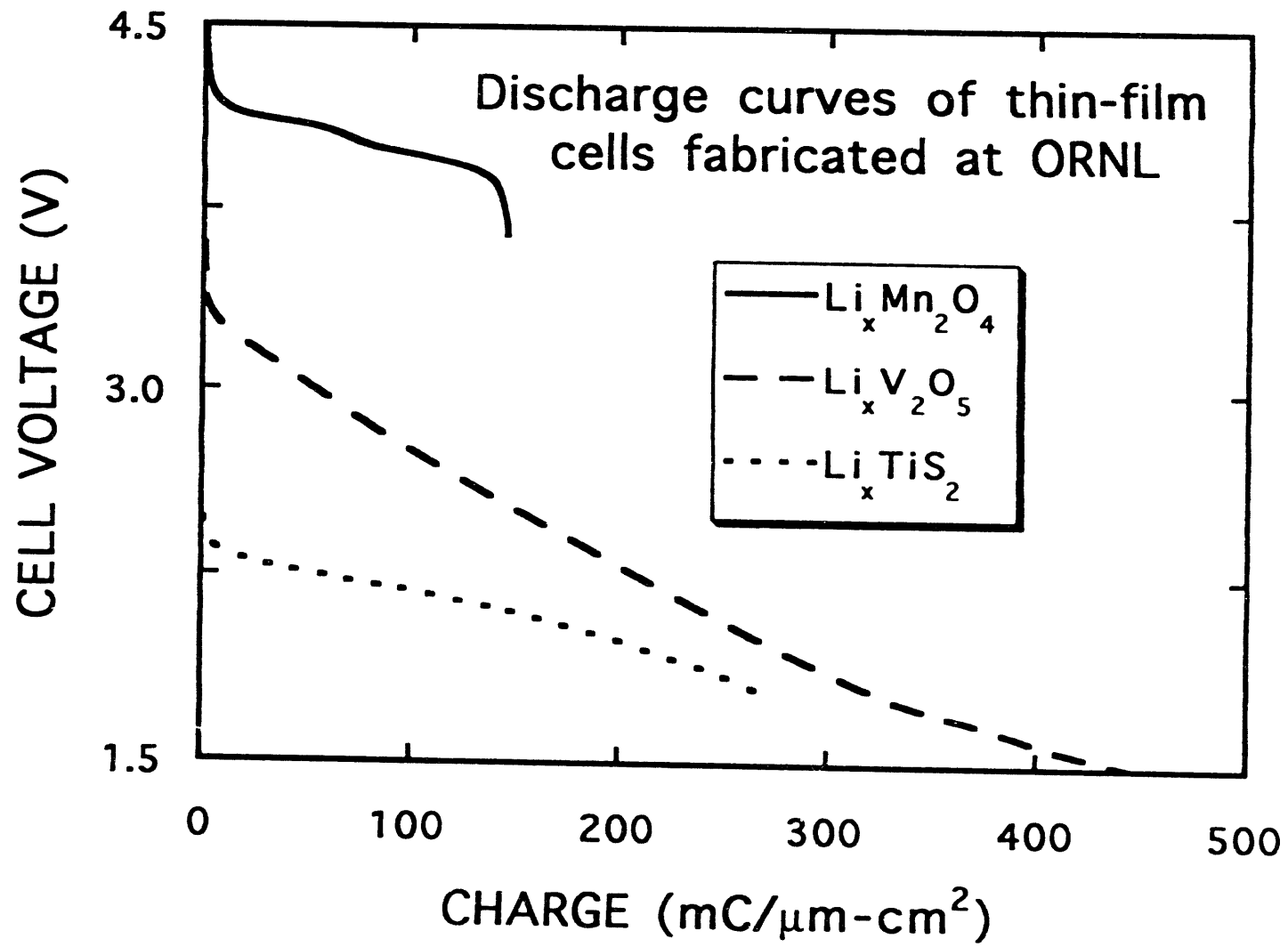


Fig. 3

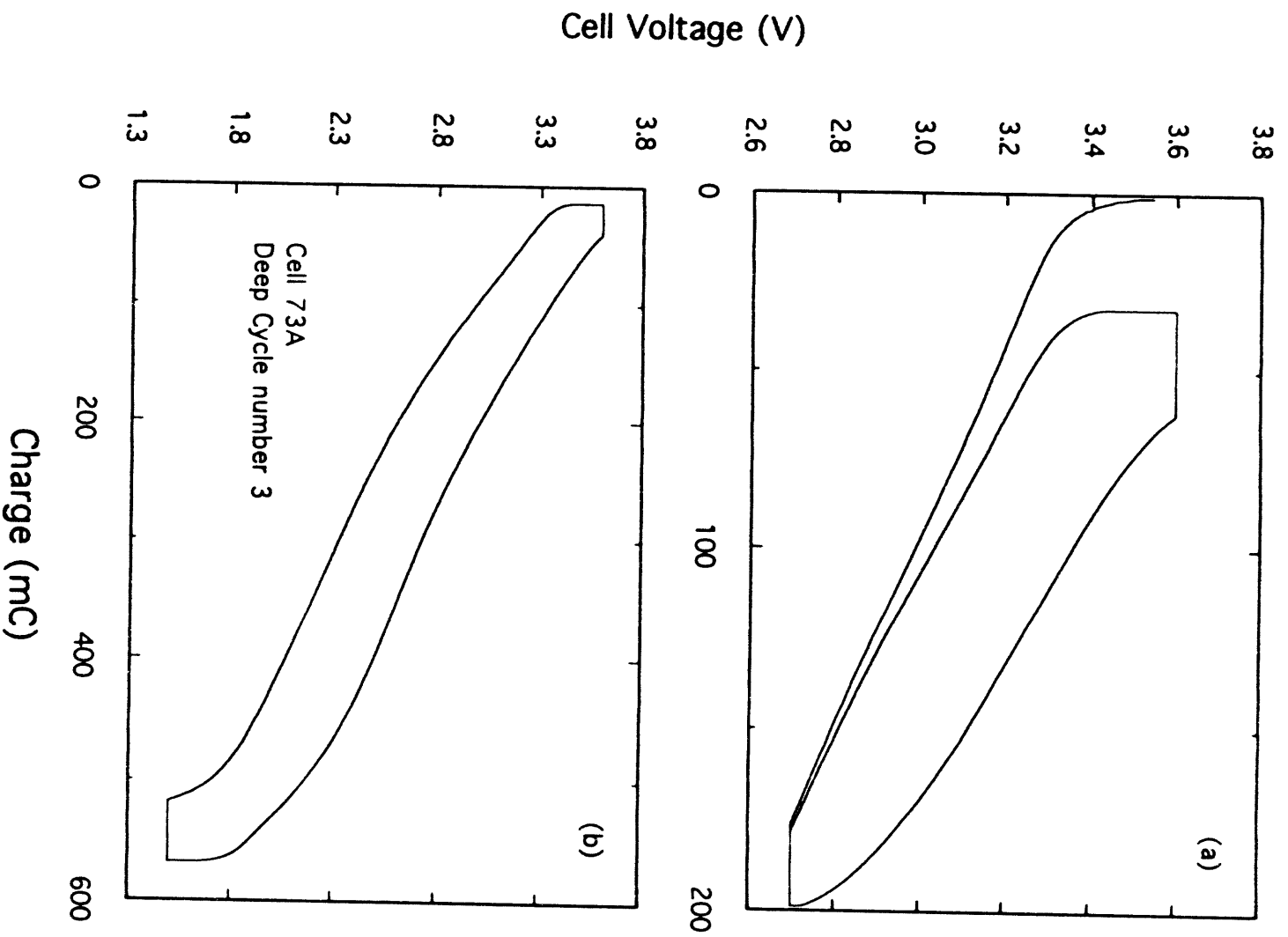


FIG. 4

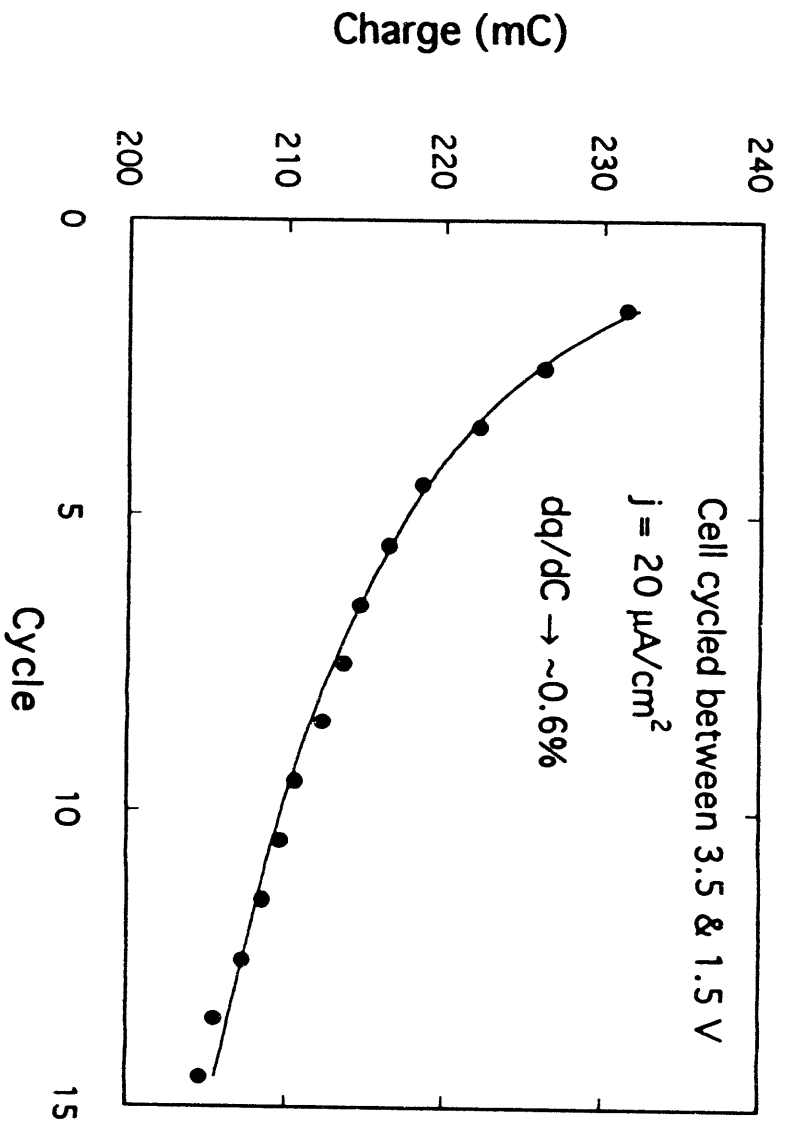


Fig. 5

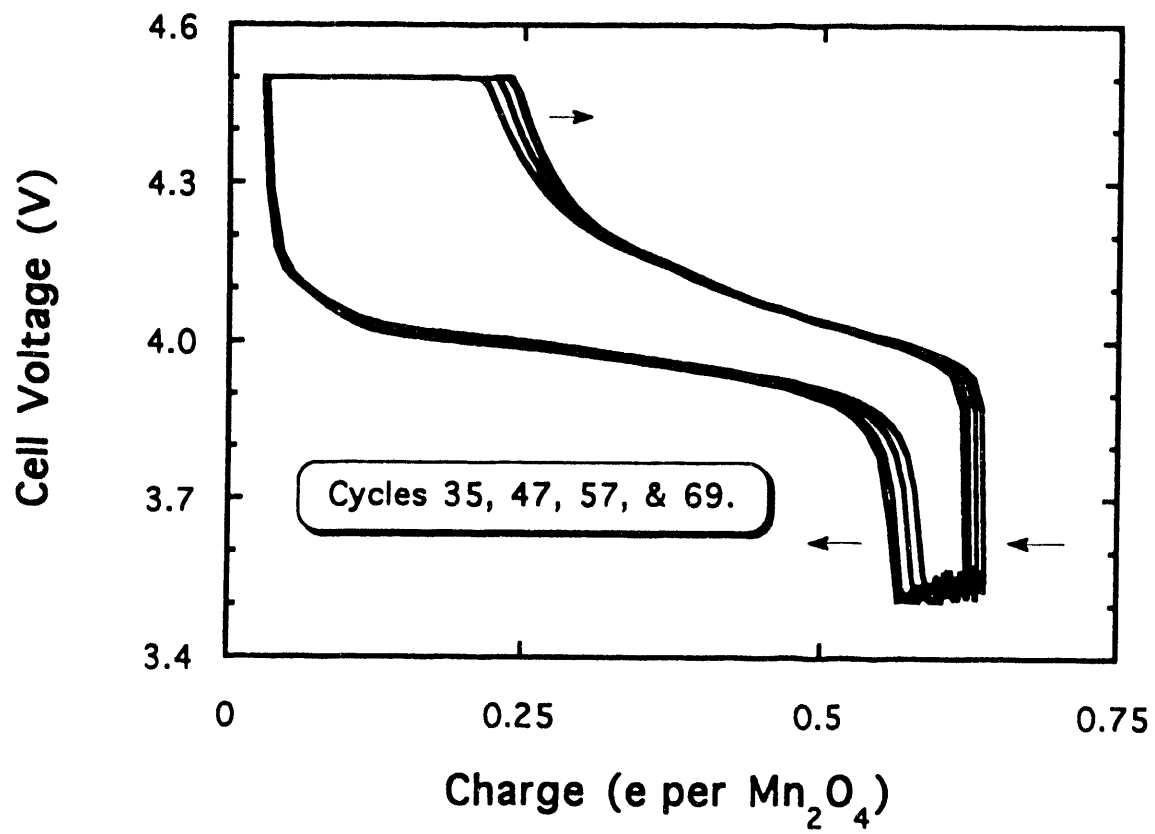


Fig. 6

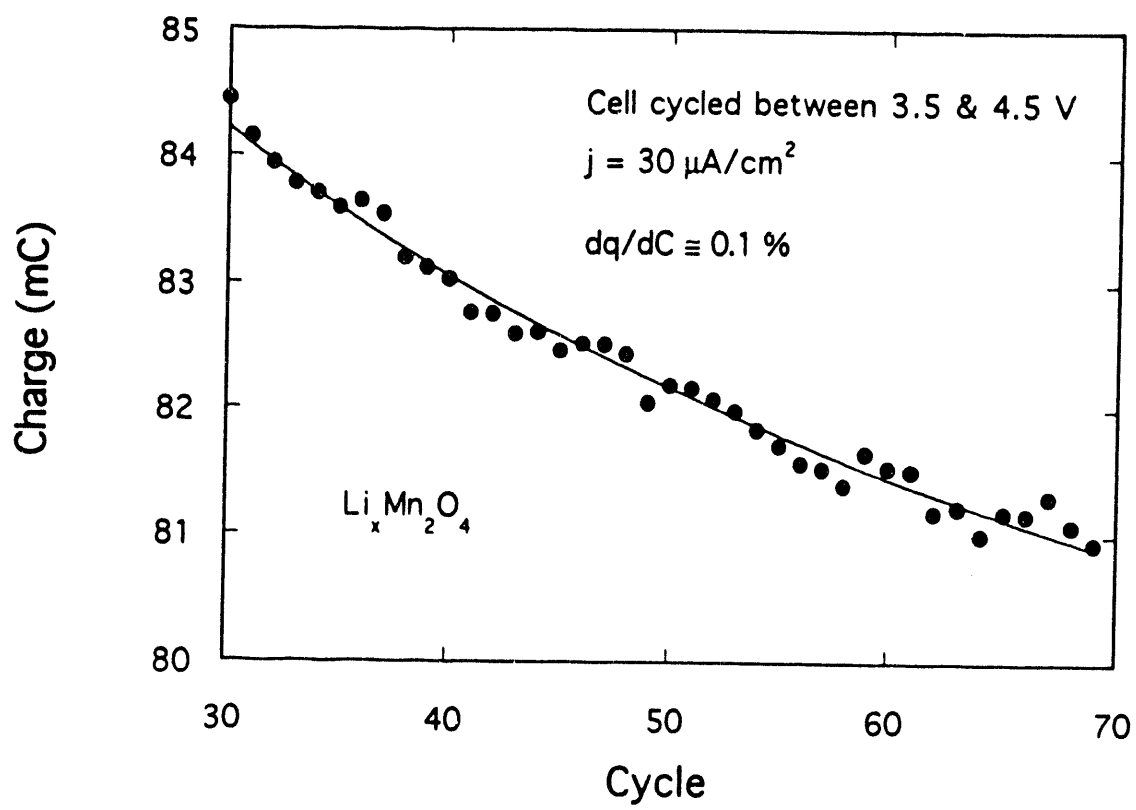


Fig. 7

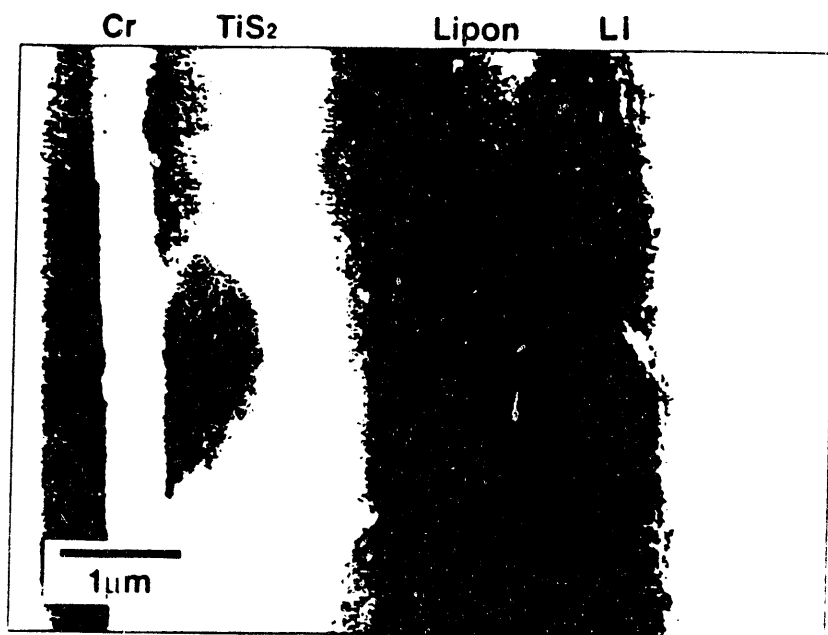


Fig. 8

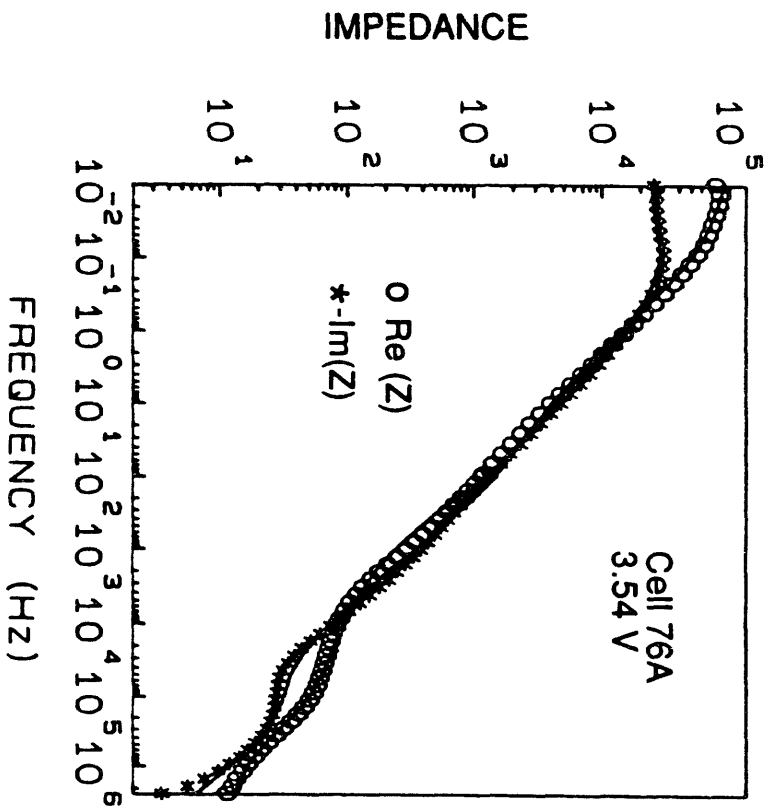
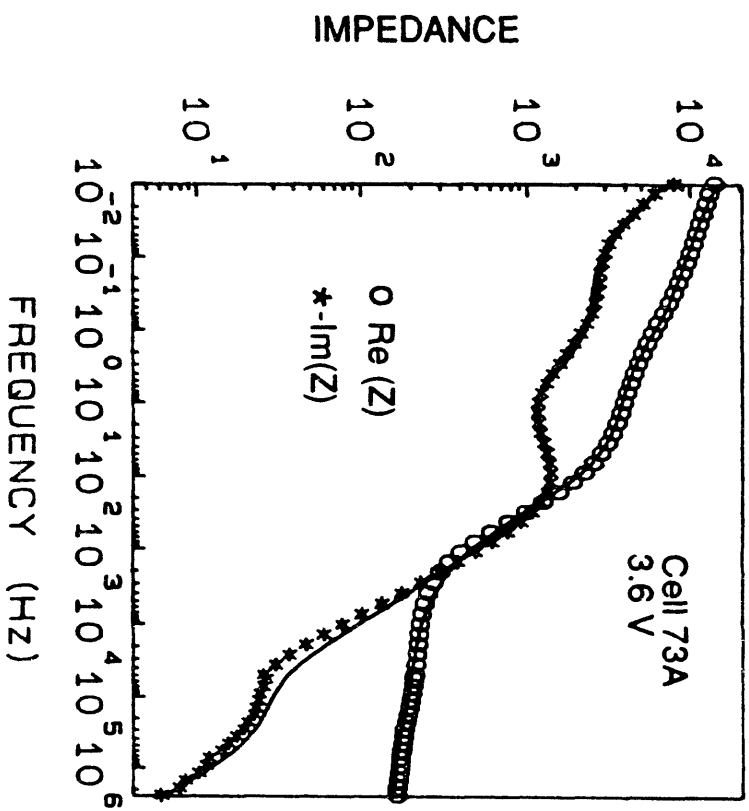


Fig. 9(a)

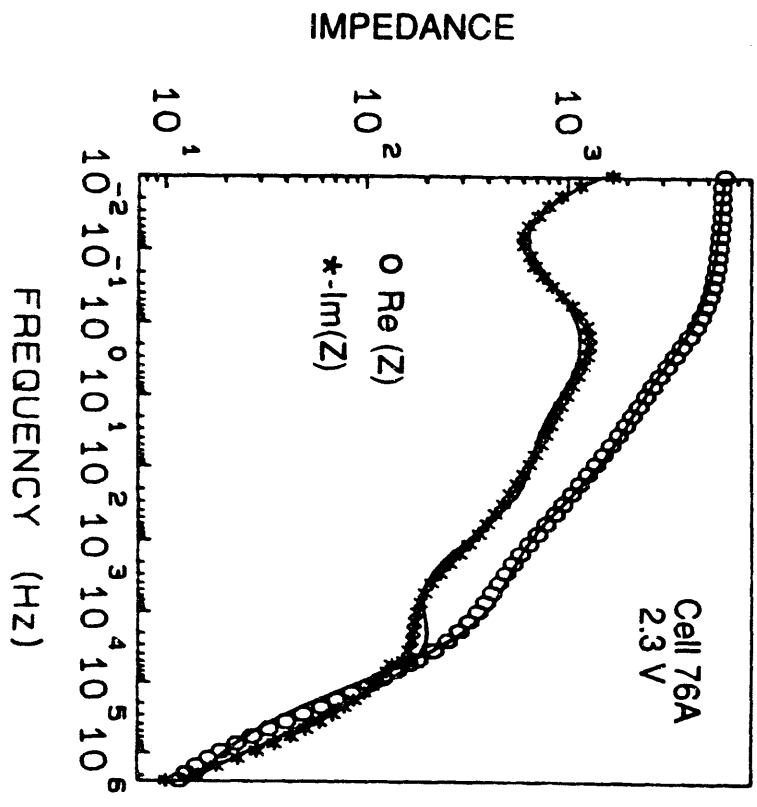
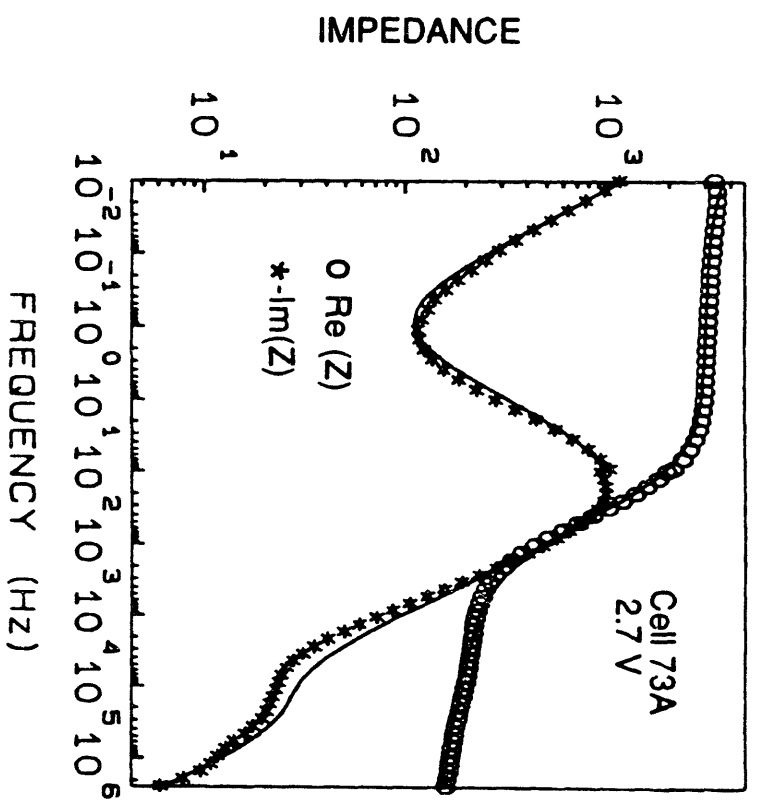


Fig. 9(b)

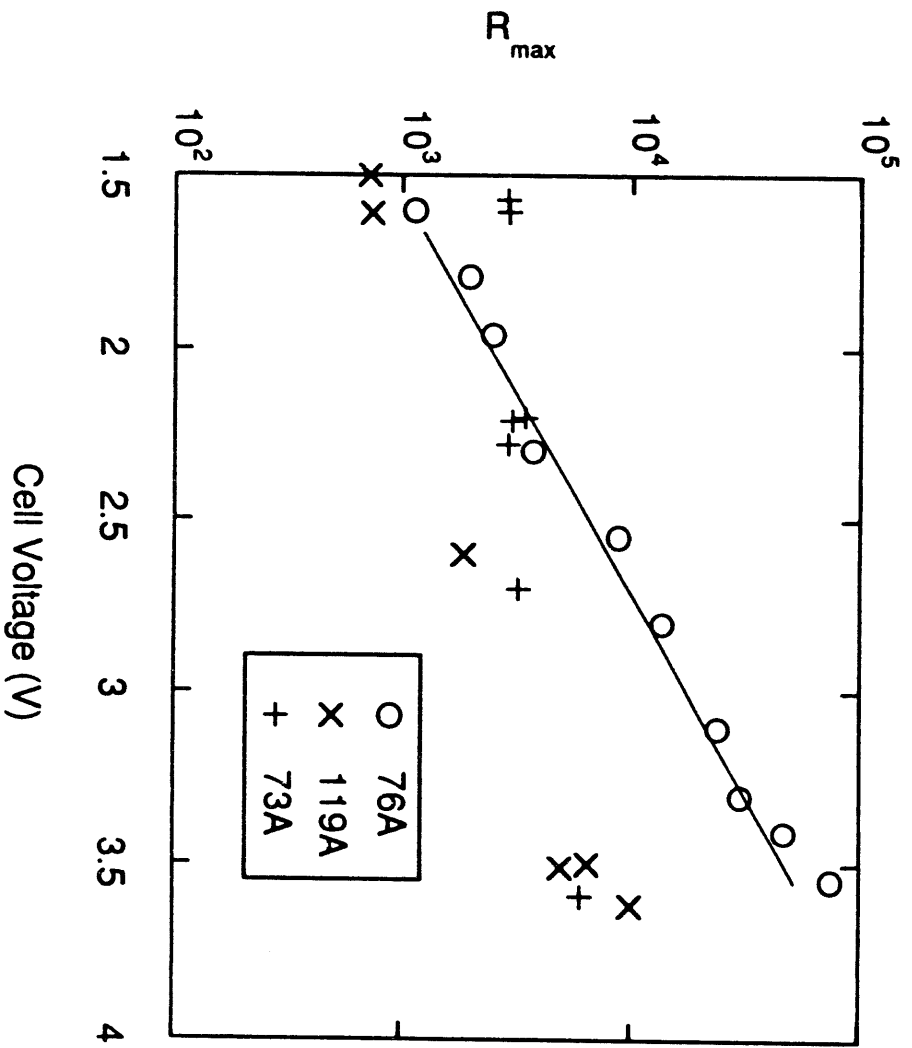


Fig. 10

**DATE
FILMED**

10 / 17 / 94

END

